# Simple Methods to Represent Shapes with Sample Spheres

Li-Yi Wei
Adobe Research

Arjun V Anand
Adobe Inc.

Shally Kumar
Adobe Inc.

Tarun Beri
Adobe Inc.

## ABSTRACT

Representing complex shapes with simple primitives in high accuracy is important for a variety of applications in computer graphics and geometry processing. Existing solutions may produce suboptimal samples or are complex to implement. We present methods to approximate given shapes with user-tunable number of spheres to balance between accuracy and simplicity: touching medial/scale-axis polar balls and k-means smallest enclosing circles. Our methods are easy to implement, run efficiently, and can approach quality similar to manual construction.

## CCS CONCEPTS

• **Computing methodologies** → **Texturing**; **Shape modeling**.

## KEYWORDS

element, sampling

## 1 BACKGROUND

Natural and man-made objects come into a variety of sizes and shapes. These geometry shapes play a central role in many scientific and engineering disciplines. Some shapes can be complex and thus challenging to store and compute. Thus, how to represent general shapes in sufficiently simple and yet accurate forms is an important research question.

Ideally, we would like to represent a given shape (e.g., a polygonal mesh model or a vector graphics design) using a small number of simple primitives (e.g., spheres) that can approximate the desired properties of the original shapes with sufficient accuracy. The definition of the latter is often application dependent, such as collision handling for physics simulation [Hubbard 1996], level of details for progressive rendering [Rusinkiewicz and Levoy 2000], shadow computation for global illumination [Wang et al. 2006], control handles for deformation [Jacobson et al. 2011; Phogat et al. 2019], or element distribution for design [Hsu et al. 2020].

Due to the importance of this problem, a variety of solutions have been proposed to approximate shapes with sample spheres
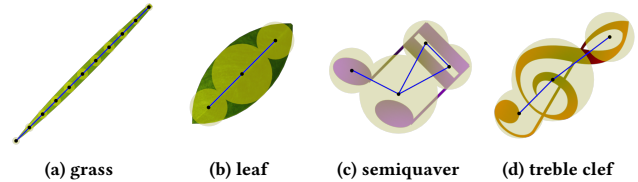
Figure 1: *Element representation.* **The black dots indicate the sample positions. The radii of the yellow circles represent the sample weights** $w_s$**. The blue lines denote the element graphs. The sampling can be sparse (a), dense (b), overlapping (c) or hybrid (d). These samples are manually placed and connected in [Hsu et al. 2020].**
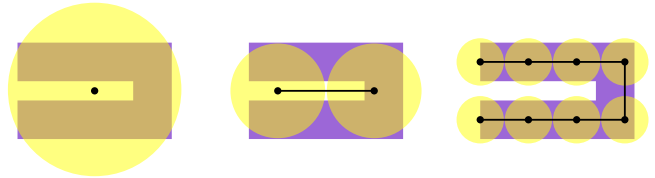


Figure 2: *Variety in element sampling.* **Depending on the design choice, the same element (purple) can be represented in different ways, such as 1 sample for a rigid component (left), 2 samples for a mildly deformable shape (middle), and 8 samples to allow further deformation among the two branches (right).**

[Stolpner et al. 2012; Thiery et al. 2013; Wang et al. 2006]. The method in [Hsu et al. 2020] lets users manually place and connect these spheres to reflect their design intention as illustrated in Figure 1 and Figure 2 that might not be divinable by automatic computation. However, it might not be reasonable to require all users to go through this process as it is more natural for them to directly design the element shapes without thinking about the underlying implementation. The Puppet Warp tool in Adobe Illustrator has a machine-learning-based method for automatic pin placement [Phogat et al. 2019], but it often produces undesirable outcomes, such missing symmetries and leaving one part of the shape inconsistent with the other (Figure 6).
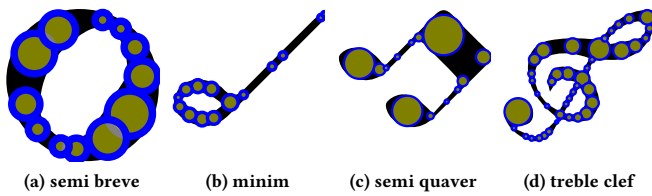
## 2 METHOD

We provide two automatic methods to sample given shapes with spheres. Both methods are very simple to implement, run fast, and can well represent the original shapes with a few spheres, whose numbers can be tuned by the users or the rest of the authoring system as a quality-performance trade off:

$\xi \leftarrow$ user specified spacing ratio $\in [0\ \infty)$
compute MAT/SAT T of a given element $e$
// [Amenta et al. 2001; Steenkamp 2019]
sample set $S \leftarrow \emptyset$
**for** *each polar ball* $b \in T$ *in decreasing radius* **do**
    *include* $\leftarrow$ *true*
    **for** *each* $b' \in S$ **do**
        **if** $\|b_{center} - b'_{center}\| < \xi \left( b_{radius} + b'_{radius} \right)$ **then**
            *include* $\leftarrow$ *false*
        **end**
    **end**
    **if** *include* **then**
        $S \leftarrow S + b$
    **end**
**end**
**return** S

**Algorithm 1:** *Element sampling via touching polar balls from a MAT/SAT tree.*



(a) semi breve     (b) minim     (c) semi quaver     (d) treble clef

**Figure 3:** *Automatic element sampling results via touching MAT/SAT polar balls.* **Users can set an upper limit on the overlap among sample spheres** $\xi$ **(for performance reason), and our method can optimize the number of samples, their locations, and weights. In this example,** $\xi = 0.8$**.**



(a) semi breve     (b) minim     (c) semi quaver     (d) treble clef
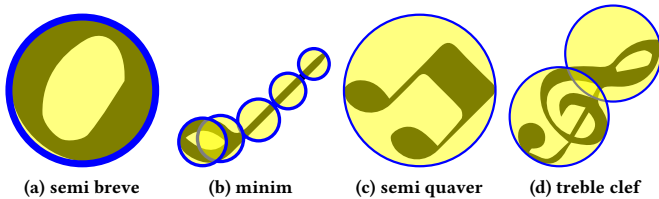
**Figure 4:** *Automatic element sampling results via k-means smallest enclosing circle.* **Users can set an upper limit on the number of samples per element (for performance reason)** $B$**, and our method can optimize the number of samples, their locations, and weights for each element. In this example,** $B = 8$**. Notice the number of samples for different elements are automatically chosen depending on their shape complexity.**

*Touching medial/scale axis polar balls (MAT).* In this method, we sample the medial/scale axis polar balls from a given shape [Amenta et al. 2001; Steenkamp 2019], and select a subset in which any two spheres overlay no more than a user selected threshold $\xi$. In our current implementation, we set a threshold of overlap

$P(e) \leftarrow$ uniform point sets from a given element $e$
$B \leftarrow$ user-specified number of samples for $e$
sample set $S \leftarrow$ random $B$ centers from $P(e)$ with 0 radii
**while** *not enough iterations* **do**
    // *compute nearest ball center for each point*
    **for** *each* $b \in S$ **do**
        $P(b) \leftarrow \emptyset$
    **end**
    **for** *each* $p \in P(e)$ **do**
        $b' = argmin_b \|p - b_{center}\|,\ \forall b \in S$
        $P(b') \leftarrow P(b') + p$
    **end**
    // *compute smallest enclosing circles*
    **for** *each* $b \in S$ **do**
        $b \leftarrow SmallestEnclosingCircle\,(P(b))$
    **end**
**end**
**return** S

**Algorithm 2:** *Element sampling via k-means smallest enclosing circles.*



(a) semi breve     (b) minim     (c) semi quaver     (d) treble clef
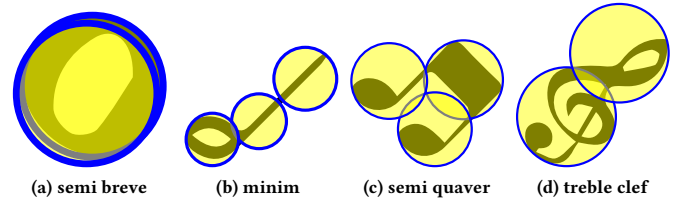
**Figure 5:** *K-means smallest enclosing circle with at least two samples per element.*

between the radii of the two spheres. For example, if the threshold is 0, no spheres can intersect. And if the threshold is $\infty$, all polar balls will be selected. We find it helpful to select the polar balls in decreasing size so ensure the larger and thus more representative ones are retained first. The method is summarized in Algorithm 1. See Figure 3 for examples.

*K-means clustering with smallest enclosing circles (SEC).* In this method, we combine k-means clustering with smallest enclosing circle [Nayuki 2018; Wikipedia 2019] to iterate the 2 steps: find the nearest ball center for each point on the element, and compute the smallest enclosing ball/circle from all belonging points (instead of the centroid step in k-means). The points can be uniformly sampled from the element boundary paths (including interior holes). The method is summarized in Algorithm 2. Users can specify a $[min, max]$ range of the number of samples for a given element, and run our algorithms to decide which number produces the minimal total sample ball areas. ($min > 1$ prevents 1-sample elements that can never deform.) See Figure 4 and Figure 5 for examples.

As can be seen, the MAT method tends to produce more spheres that all fit within the original shapes, while the SEC method tends to produce less spheres that cover the original shapes. Thus, they are more suitable for deformable and rigid elements, respectively.

*Graph construction.* After placing the samples, we can connect them to form element graphs (Figure 1 and Figure 2). For a fully rigid shape, we can connect all pairs of samples to form a complete graph. To allow (skeletal) deformation, we can connect along the medial/scale axis for MAT or overlapping/touching sample spheres for SEC.

## 3 REFINEMENT
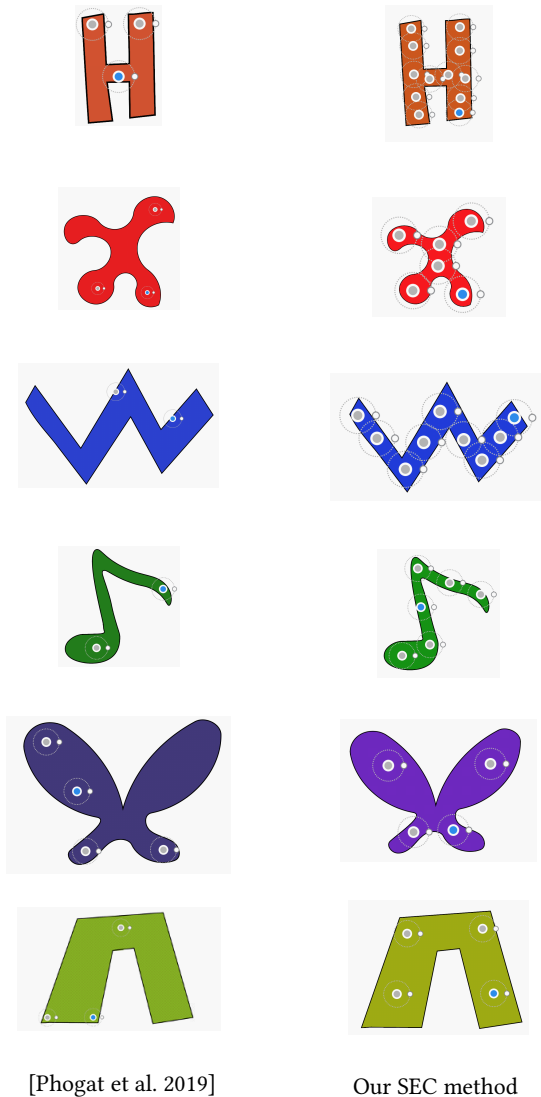


[Phogat et al. 2019]          Our SEC method

**Figure 6: *Comparison with Adobe Illustrator Puppet Warp automatic pin placement [Phogat et al. 2019].* The results for [Phogat et al. 2019] were directly screen-captured and thus have different rendering effects from our results. Notice that the samples produced via [Phogat et al. 2019] might miss key parts of the shapes, while our results can provide more balanced coverage.**

The SEC method in Section 2 can produce unpredictable results due to random initialization (e.g., comparing Figure 4b and Figure 5b). We describe a better initialization method and more principled criteria for choosing the number of samples.

*Objectives.* The desired sampling should satisfy the following goals:

(1) Sample centers should lie on, or close to, the medial axis of the input shape.
(2) Overlap among samples should be minimal.
(3) Samples should occupy minimum external area (i.e., area outside the input shape), but maximum internal area.
(4) There should be a low number of adjacent samples. One adjacent sample (for every sample) is okay, two are good if they lie on opposite sides, more than two are only desired in 'T' or '+' like shapes.
(5) Samples should symmetrically cover the shape, i.e., samples with left side outside the shape while right side inside the element are less preferred, while samples completely inside or equivalently outside on left/right and top/bottom are more preferred.

Some of the criterion mentioned above might work against each other. Let us consider the case of a narrow $U$ shaped element versus a wider one. If the parallel boundary walls of the element are far apart, then having a sample center at the medial axis would mean large samples. This could increase the external area they occupy. Thus, point 1 might work against point 3. On the other hand, if we reduce the size of samples (and keep their centers at medial axis), it could reduce the external area but violate adjacencies. Thus, we do not directly enforce keeping sample centers at medial axis and rather achieve that as a side-effect of other criteria. We keep the external area low, maintain desired adjacency and symmetry to enforce sample centers to be as close to the medial axis as possible.

*Initialization.* The k-means clustering in the SEC method requires a set of points to operate with. Random initialization can produce unstable results; each time we execute sampling, a different result is returned. To meet our first objective, we place points uniformly along the boundary and randomly in the interior of the input shape, and sort all the points first on y-axis and then on x-axis. From this sorted point set, we pick up uniformly separated points (like rejection sampling for dart throwing [Yuksel 2015]) for initialization. This always produces stable results and has the tendency to converge faster.

*Optimizing sample count.* Let $D_A$ be the area of the input shape and $r_{min}$ be the radius $w_s$ of the smallest sample that we would like to create. If $D_A$ is less than the area of the smallest possible sample $S_{A_{min}}$ (i.e., $\pi r_{min}{}^2$), we treat that as a special case. We can either rescale the shape or create one tight fitting sample (ignoring $r_{min}$) located at the center of the shape. Otherwise, we use the following algorithm to determine the number and locations of samples.

We first find the minimum and maximum possible number of samples. Minimum count ($N_{min}$) is default to 1 and maximum count ($N_{max}$) is computed as $\lfloor \frac{D_A}{S_{A_{min}}} \rfloor$. We linearly scan all possibilities from $N_{min}$ to $N_{max}$ and find the number of samples that gives us the minimum cost, defined in Equation (1). At every step (in the search

space $N_{min}$ to $N_{max}$), we perform the SEC method (Algorithm 2), and calculate the following energy value to identify the minimum that indicates the desired sample count:

$$C = w_o M_o + w_e M_e + w_a M_a + w_y M_y \qquad (1)$$

, where the subscripts $o$, $e$, $a$ and $y$ represent overlap, exterior area, adjacency, and asymmetry, w and $M$ represent weight and measure of the subscripted entities. We normalize all measures on an equivalent scale $[0\ 1]$ to avoid results being skewed towards any term.

$M_o$ is computed as total overlapping area of all samples divided by total area of all samples. Since all samples are circles, this is straight forward to compute. Note that if two samples overlap, we count the overlapping area in both samples.

$M_e$ is computed as the ratio of total area of samples not inside the shape to the total area of samples. Note that we do not deal with overlaps here. For every sample, we just compute how much of it is outside the shape. This requires circle and triangle intersection evaluations which we perform via triangle tessellation of the input shape.

$M_a$ is computed by finding the number of samples that are overlapping or adjoining. If a sample has radius $r_1$ and another has radius $r_2$ and the separation between their centers is less than $r_1 + r_2$, we count that as an adjacency. We also use some epsilon tolerance for stable results. The extreme case is that every sample is adjacent to every other sample. Thus, for $N$ samples, the maximum possible number of adjacencies $A_{max}$ is given by $N(N-1)$ and for a linearly connected sampling (like in a leaf shape in Figure 1b), the desired number of adjacencies $A_{min}$ is given by $2(N-1)$. Thus, we can compute $M_a$ as following:

$$M_a = \frac{|A - A_{min}|}{A_{max}} \qquad (2)$$

, where $A$ is the total count of adjacencies among all samples. Note that if two samples are adjacent, we count adjacency from both sides. Since it will be rare to have $A_{max}$ adjacencies in a practical setup, there will be a higher tendency to have $M_a$ less than $M_o$, $M_e$ and $M_y$. Thus, to counter this, we do two things: use $3(N-1)$ as a practical upper bound for $A_{max}$, and set $w_a$ higher than $w_o$, $w_e$ and $w_y$. Also note that $M_a$ is mostly immaterial (being zero) when number of samples is 2. Thus, in that scenario, we ignore $M_a$ and evaluate cost $C$ by considering the other three measures only.

$M_y$ is computed by dividing every sample into four quadrants and measuring how much asymmetric coverage is exhibited by opposite quadrants (quadrant 1 versus 3 and quadrant 2 versus 4; quadrants are numbered anti-clockwise from x-axis). We find the number of interior pixels $p$ in each of the four quadrants and use the following formula to find $M_y$:

$$M_y = \frac{0.5|p_1 - p_3| + 0.5|p_2 - p_4|}{Q} \qquad (3)$$

, where $Q$ represents area of a quadrant; $p_1$, $p_2$, $p_3$ and $p_4$ represent interior pixels (i.e. inside the element) in quadrants 1, 2, 3 and 4.

*Band normalization.* Different measures ($M_o$, $M_e$, $M_a$ and $M_y$) can have different range of values. Specifically, $M_a$ tends to have lower absolute values than others. On the other hand, the weights ($w_o$, $w_e$, $w_a$ and $w_y$) associated with these measures are defined to establish their relative importance and they are going to behave correctly only when the values of measures are on an equivalent scale. Thus, we *band normalize* all the measures before computing the final cost. For *band normalization*, we divide each measure by its average value across all runs from $N_{min}$ to $N_{max}$. We perform *band normalization* separately from normalizing all measures to $[0\ 1]$ range. However, it is possible to combine both these in a single step.

Figure 6 compares [Phogat et al. 2019] with our refined SEC method.

## 4 CONCLUDING REMARKS

We describe simple methods to represent given shapes with sample spheres. We have evaluated our methods for 2D vector graphics applications including element synthesis [Hsu et al. 2020] and shape warping [Phogat et al. 2019], and plan to explore applications in 3D modeling. We also plan to perform more comprehensive analysis and comparisons against other methods.

## REFERENCES

Nina Amenta, Sunghee Choi, and Ravi Krishna Kolluri. 2001. The Power Crust. In *SMA '01* (Ann Arbor, Michigan, USA). 249–266.

Chen-Yuan Hsu, Li-Yi Wei, Lihua You, and Jian Jun Zhang. 2020. Autocomplete Element Fields. In *CHI '20*. 1–13.

Philip M. Hubbard. 1996. Approximating Polyhedra with Spheres for Time-Critical Collision Detection. *ACM Trans. Graph.* 15, 3 (1996), 179–210.

Alec Jacobson, Ilya Baran, Jovan Popović, and Olga Sorkine. 2011. Bounded Biharmonic Weights for Real-Time Deformation. *ACM Trans. Graph.* 30, 4, Article 78 (2011), 8 pages.

Project Nayuki. 2018. Smallest enclosing circle.

Ankit Phogat, Matthew Fisher, Danny M. Kaufman, and Vineet Batra. 2019. Skinning Vector Graphics with GANs. In *ACM SIGGRAPH 2019 Posters* (Los Angeles, California). Article 70, 2 pages.

Szymon Rusinkiewicz and Marc Levoy. 2000. QSplat: A multiresolution point rendering system for large meshes. In *SIGGRAPH '00*. 343–352.

Floris Steenkamp. 2019. Medial (and Scale) Axis Transform library - SVG focused.

Svetlana Stolpner, Paul Kry, and Kaleem Siddiqi. 2012. Medial Spheres for Shape Approximation. *IEEE Trans. Pattern Anal. Mach. Intell.* 34, 6 (2012), 1234–1240.

Jean-Marc Thiery, Émilie Guy, and Tamy Boubekeur. 2013. Sphere-Meshes: Shape Approximation Using Spherical Quadric Error Metrics. *ACM Trans. Graph.* 32, 6, Article 178 (2013), 12 pages.

Rui Wang, Kun Zhou, John Snyder, Xinguo Liu, Hujun Bao, Qunsheng Peng, and Baining Guo. 2006. Variational Sphere Set Approximation for Solid Objects. *Vis. Comput.* 22, 9 (2006), 612–621.

Wikipedia. 2019. Smallest-circle problem.

Cem Yuksel. 2015. Sample Elimination for Generating Poisson Disk Sample Sets. *Comput. Graph. Forum* 34, 2 (2015), 25–32.